Asaroidoxazines from the Roots of *Asarum asaroides* Induce Apoptosis in Human Neuroblastoma Cells

Shinji Ohta,[*,†] Shiori Oshimo,[‡] Emi Ohta,[†] Tatsuo Nehira,[†] Hisashi Ômura,[†] Mylene M. Uy,[§] and Yasuhiro Ishihara[*,†]

[†] *Graduate School of Integrated Sciences for Life, Hiroshima University, 1-7-1 Kagamiyama, Higashi-Hiroshima 739-8521, Japan*

[‡] *Graduate School of Biosphere Science, Hiroshima University, 1-7-1 Kagamiyama, Higashi-Hiroshima 739-8521, Japan*

[§] *Department of Chemistry, Mindanao State University-Iligan Institute of Technology, Iligan City 9200, Philippines*

ABSTRACT: Plants in the family Aristolochiaceae contain phenanthrene skeleton-containing chemical constituents that exhibit nephrotoxic, carcinogenic, mutagenic, anti-inflammatory, and cytotoxic effects. Two new phenanthrene-containing 1,2-oxazin-6-ones, designated as asaroidoxazine A (**1**) and asaroidoxazine B (**2**), and a known aristolactam, 5-methoxyaristololactam I (**3**), were isolated from the roots of *Asarum asaroides*. The structures of compounds **1** and **2** were determined using spectroscopic methods and X-ray crystallography. Treatment of SH-SY5Y human neuroblastoma cells with 1 μM of asaroidoxazine A (**1**) induced nuclear condensation as well as caspase-3/7 activation, indicating that this compound is a strong apoptosis inducer in neuronal cells. This is the first report of apoptosis induction by phenanthrene-containing oxazines.

Asarum asaroides (C. Morren & Decne.) Makino (Aristolochiaceae), an evergreen perennial herb, is an endemic species in Japan.[1,2] Previous reports on the chemical constituents of the plant are limited, but these include the identification of volatile oil constituents,[3] anthocyanins,[2] and aristolochic acid I.[4] Derivatives of the phenanthrene skeleton-containing aristolochic acid and aristolactam are found in species of the Aristolochiaceae.[5,6] These derivatives exhibit nephrotoxic,[7,8] carcinogenic,[9] mutagenic,[10] anti-inflammatory,[11] and cytotoxic effects.[12,13]

In the course of our studies on biologically active compounds from plants,[14,15] two new phenanthrene-containing 1,2-oxazin-6-ones, designated as asaroidoxazine A (**1**) and asaroidoxazine B (**2**), in addition to a known aristolactam, 5-methoxyaristololactam I (**3**)[16] were isolated from the roots of *A. asaroides* (Figure 1). It was demonstrated that these compounds cause neurotoxicity in SH-SY5Y human neuroblastoma cells. Herein, are reported the isolation, structural elucidation, and potential biological impact of the isolated compounds.

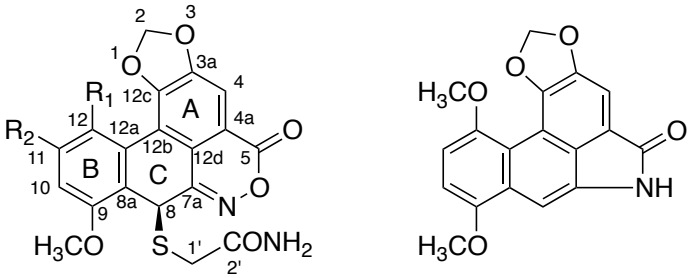

1 $R_1 = OCH_3$, $R_2 = H$

2 $R_1 = H$, $R_2 = OCH_3$

3

Figure 1. Structures of compounds **1**–**3**.

RESULTS AND DISCUSSION

The roots of *A. asaroides* were cut into small pieces and extracted with MeOH. The MeOH extract was then partitioned with hexane, and the resultant MeOH layer, after removal of the solvent, was partitioned with EtOAc and H_2O. The EtOAc-soluble material was repeatedly separated on a silica gel column to isolate compounds **1**–**3**.

Table 1. ^{1}H (500 MHz) and ^{13}C (125 MHz) NMR Data for Compounds 1 and 2 in $CDCl_3$

	1		**2**	
no.	δ_C, type	δ_H (*J* in Hz)	δ_C, type	δ_H (*J* in Hz)
2	102.5, CH_2	6.21, d (0.9)	103.1, CH_2	6.30, d (0.9)
		6.35, d (0.9)		6.42, d (0.9)
3a	153.9, C		153.4, C	
4	105.4, CH	7.59, s	106.4, CH	7.65, s
4a	118.6, C		119.2, C	
5	163.4, C		163.3, C	
7a	152.3, C		152.0, C	
8	39.0, CH	5.48, s	38.7, CH	5.47, s
8a	121.0, C		111.9, C	
9	150.5, C		157.7, C	
10	113.2, CH	7.03, d (9.2)	99.8, CH	6.59, d (2.3)
11	113.1, CH	7.02, d (9.2)	161.4, C	
12	151.5, C		104.5, CH	7.54, d (2.3)
12a	118.0, C		128.9, C	
12b	111.7, C		114.9, C	
12c	150.6, C		149.8, C	
12d	119.7, C		118.2, C	
1'	34.7, CH_2	3.09, d (16.9)	34.3, CH_2	3.08, d (16.9)
		3.48, d (16.9)		3.59, d (16.9)
2'	170.4, C		170.6, C	
NH		5.69, br s		5.55, br s
		6.96, br s		6.95, br s
OMe-9	56.6, CH_3	3.95, s	56.2, CH_3	3.97, s
OMe-11			55.6, CH_3	3.89, s
OMe-12	56.3, CH_3	3.89, s		

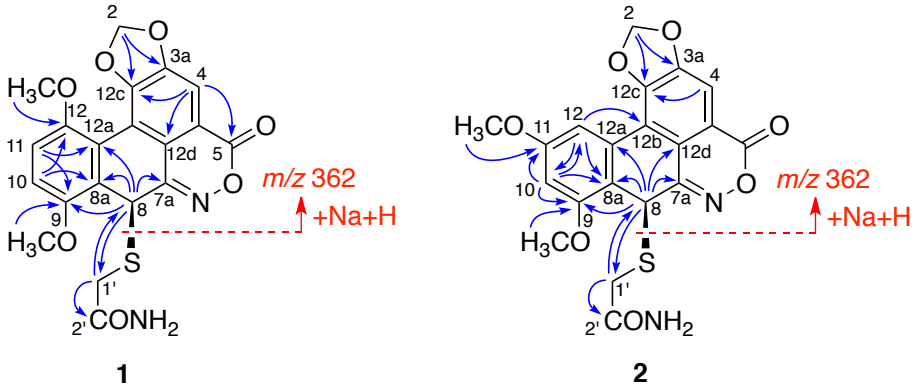

1 2

Figure 2. Key HMBC correlations and positive-ion ESIMS/MS analysis (precursor ion: *m/z* 451 $[M + Na]^+$) for **1** and **2**.

Compound **1** was obtained as pink crystals and exhibited $[M + Na]^+$ and $[M - H]^-$ ions at *m/z* 451 and 427 in the positive- and negative-ion ESIMS spectra, respectively (Figures S6 and S9, Supporting Information). The positive-ion HRESIMS analysis {*m/z* 451.0572 ($[M + Na]^+$; calcd for $C_{20}H_{16}N_2O_7SNa^+$, 451.0570)}, established the molecular formula of **1** as $C_{20}H_{16}N_2O_7S$ (Figure S7, Supporting Information). This compound was negative when treated with bromocresol green spray on TLC and did not react with diazomethane, indicating the absence of a carboxyl group. The IR absorption bands at 3430, 1727, 1664, 1631, 1590, 1490, and 1472 cm^{-1} suggested the presence of NH, C=O, C=N, C=C functionalities. The UV (MeOH) absorption maxima at 210 (log ε 4.64) and 277 nm (log ε 4.35) implied the presence of a dihydrophenanthrene skeleton,[17] which was supported by the ^1H and ^{13}C NMR data [δ_H 7.02 (1H, d, J = 9.2 Hz, H-11), 7.03 (1H, d, J = 9.2 Hz, H-10), 7.59 (1H, s, H-4); δ_C 111.7 (C-12b), 150.6 (C-12c), 153.9 (C-3a), 105.4 (C-4), 118.6 (C-4a), 119.7 (C-12d), 118.0 (C-12a), 121.0 (C-8a), 150.5 (C-9), 113.2 (C-10), 113.1 (C-11), 151.5 (C-12), 152.3 (C-7a), 39.0 (C-8)] (Table 1; Figures S1 and S2, Supporting Information).

The ^{1}H and ^{13}C NMR spectra also revealed the presence of two additional carbonyl carbon atoms at δ_C 163.4 (C-5) and 170.4 (C-2'), a dioxymethylene [δ_H 6.21 (1H, d, J = 0.9 Hz, H-2), 6.35 (1H, d, J = 0.9 Hz, H-2); δ_C 102.5], a heteroatom-substituted methylene [δ_H 3.09 (1H, d, J = 16.9 Hz), 3.48 (1H, d, J = 16.9 Hz); δ_C 34.7], and two methoxy groups [δ_H 3.89 (3H, s), 3.95 (3H, s); δ_C 56.3, 56.6]. The HMBC correlations from the dioxymethylene protons (δ_H 6.21 and 6.35) to the two sp^2 carbons [δ_C 153.9 (C-3a) and 150.6 (C-12c)] and from the downfield singlet proton at δ_H 7.59 (1H, s, H-4) to the carbonyl carbon [δ_C 163.4 (C-5)] and the sp^2 carbons [δ_C 150.6 (C-12c), and 119.7 (C-12d)] indicated that a methylenedioxy substituent and one of the carbonyl carbons are attached to ring A (Figures 2 and S5, Supporting Information). The HMBC correlations from the two methoxy groups [δ_H 3.89 (3H, s) and 3.95 (3H, s)] to the two sp^2 carbons [δ_C 151.5 (C-12) and 150.5 (C-9), respectively] and from the two *ortho*-protons [δ_H 7.02 (1H, d, J = 9.2 Hz, H-11) and 7.03 (1H, d, J = 9.2 Hz, H-10)] to the sp^2 carbons [δ_C 118.0 (C-12a)/150.5 (C-9) and 121.0 (C-8a)/151.5 (C-12), respectively] indicated that ring B has *p*-dimethoxy substituents. The HMBC correlations from the downfield methylene protons [δ_H 3.09 (1H, d, J = 16.9 Hz, H-1'), 3.48 (1H, d, J = 16.9 Hz, H-1')] to C-8 and the remaining carbonyl carbon [δ_C 170.4 (C-2')] indicated the presence of a carbamoylmethylthio group and its attachment to C-8 through a thioeter linkage. The positive-ion ESIMS/MS confirmed this, as a fragment ion peak at *m/z* 362 $[M + Na - 89]^+$ (precursor: *m/z* 451 $[M + Na]^+$) was observed (Figures 2 and S8, Supporting Information). The structure of **1** was confirmed by X-ray crystallographic analysis (Figure 3). From the anomalous dispersion of the sulfur atoms, the absolute configuration of **1** was confirmed to be 8*S*, with the Flack parameter[18,19] refined to 0.05 (3). Compound **1** has a slightly distorted phenanthrene ring, in which the two aromatic rings (A- and B-rings) intersect at an angle of ~20˚. The central six-membered ring (C-ring) adopts the pseudo half-chair conformation, considerably flattened at one

end with the pseudoaxial carbamoylmethylthio substituent. In the crystal, the amide NH_2 at C-2' of **1** was intramolecularly hydrogen-bonded to the oxygen atom of the methoxy group at C-9 and intermolecularly hydrogen-bonded to the oxygen atom of the solvent molecule (MeOH). In turn, the hydroxy group of MeOH was linked to the carbonyl group at C-2' of the acetamide unit of another molecule of **1** through an intermolecular hydrogen bond to form polymeric chains along the *b* axis (Figure 4). Consequently, **1** was assigned as (*S*)-2-((9,12-dimethoxy-5-oxo-5,8-dihydro[1,3]dioxolo[4',5':3,4]phenanthro[10,1-*cd*][1,2]oxazin-8-yl)thio)acetamide, to which the name asaroidoxazine A has been given.

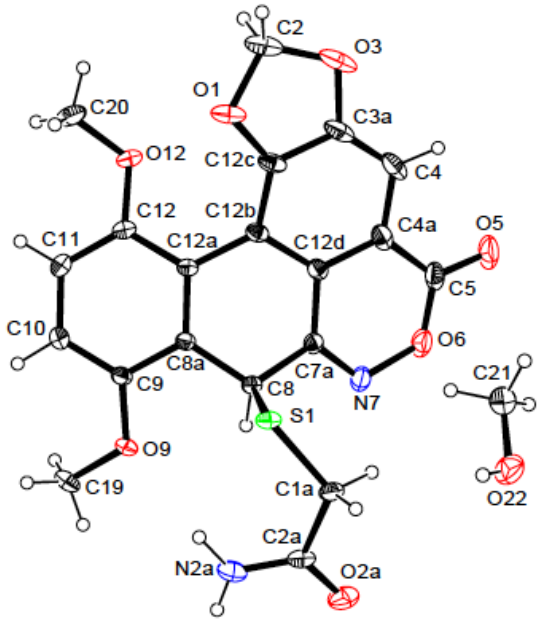

Figure 3. ORTEP diagram of **1**.

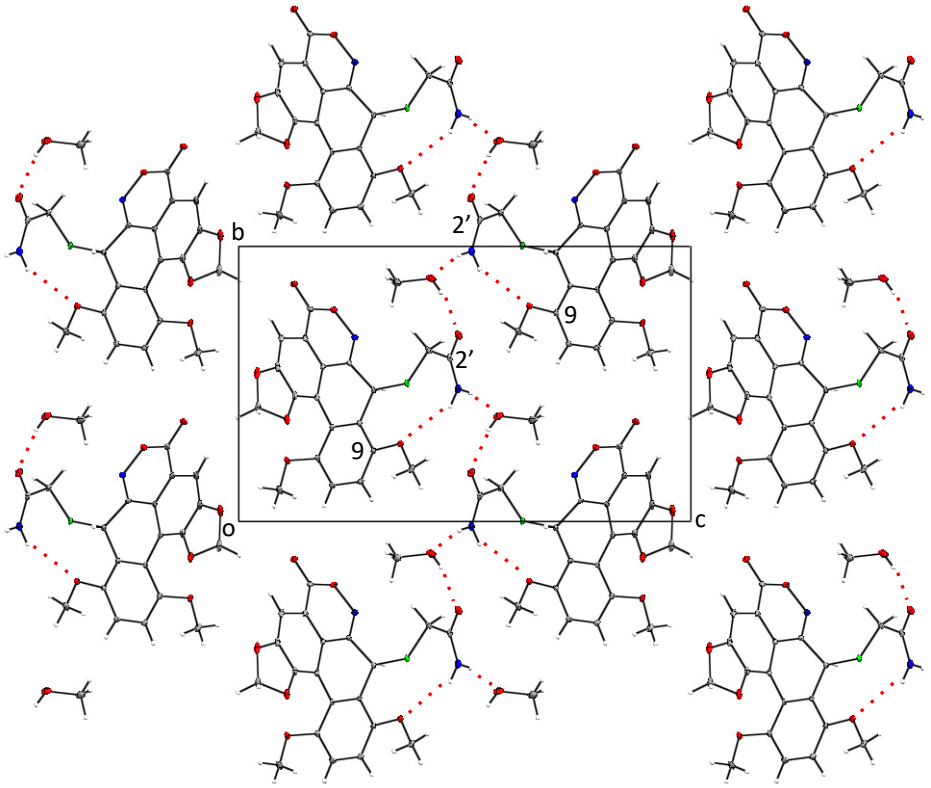

Figure 4. A diagram, viewed down the *a* axis, showing the hydrogen bonding in **1**, marked as red dashed lines.

Compound **2** was obtained as a pale yellow oil, and its molecular formula was determined to be $C_{20}H_{16}N_2O_7S$ by positive-ion HRESIMS analysis {*m/z* 451.0569 ($[M + Na]^+$; calcd for $C_{20}H_{16}N_2O_7SNa^+$, 451.0570)}, indicating **2** to be an isomer of **1** (Figure S16, Supporting Information). The ^1H and ^{13}C NMR spectra for **2** were very similar to those of **1**, except for the presence of the two *meta*-coupled aromatic protons at δ_H 6.59 (d, J = 2.3 Hz) and 7.54 (d, J = 2.3 Hz) in **2** instead of the two *ortho*-coupled aromatic protons in **1** (Table 1; Figures S10 and S11, Supporting Information). The HMBC correlations from H-8 [δ_H 5.47 (s)] to C-9 (δ_C 157.7), from H-10 [δ_H 6.59 (d, J = 2.3 Hz)] to C-8a (δ_C 111.9), C-9 (δ_C 157.7), C-11 (δ_C 161.4), and C-12 (δ_C 104.5), and from H-12 [δ_H 7.54 (d, J = 2.3 Hz)] to C-8a, C-10, and C-12b (δ_C 114.9) indicated that ring B of **2** has 9,11-dimethoxy substituents (Figures 2 and S14, Supporting Information). The

ECD spectrum [Δε 217 (–26.4), 288 (+12.9), 343 nm (–3.4)] and the specific rotation value {$[\alpha]^{25}_{D}$ +69 (*c* 0.01, $CHCl_3$)} of **2** were almost indistinguishable with those of **1** {Δε 218 (–25.8), 290 (+19.7), 344 nm (–2.1); $[\alpha]^{25}_{D}$ +147 (*c* 0.02, $CHCl_3$)}, indicating that the absolute configuration of **2** was identical to that of **1**. Consequently, **2** was established as (*S*)-2-((9,11-dimethoxy-5-oxo-5,8-dihydro[1,3]dioxolo[4',5':3,4]phenanthro[10,1-*cd*][1,2]oxazin-8-yl)thio)acetamide, to which the name asaroidoxazine B has been given.

Compound **3** was identified as 5-methoxyaristololactam I based on a comparison of the spectroscopic data with those described in the literature.[16] The structure of **3** was confirmed by X-ray crystallography (Figure 5). In the solid state, the molecules of **3** were linked to one another via intermolecular hydrogen bonds between C=O and N-H of the lactam. The dimeric structures were stabilized by the π–π stacking interactions between the phenanthrene rings (Figure 6). The interplanar spacing between the parallel phenanthrene skeletons was ~3.5 Å, typical for the π–π stacking between aromatic rings.[20,21]

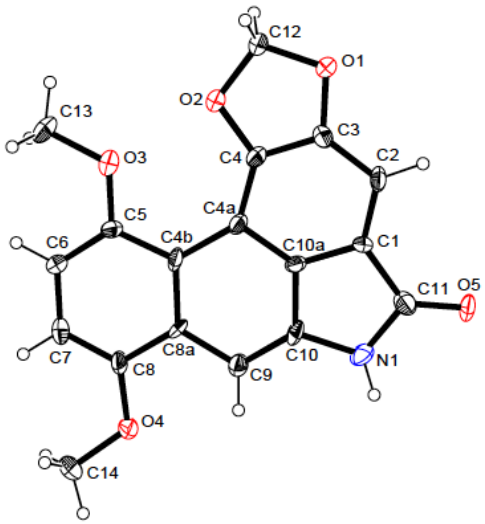

Figure 5. ORTEP diagram of **3**.

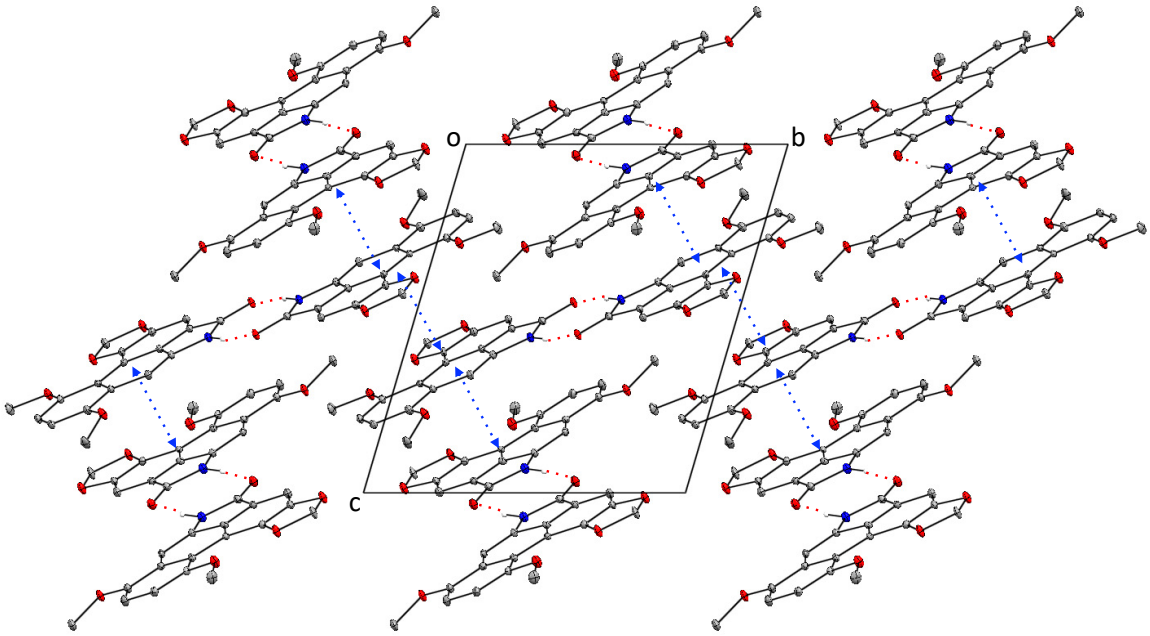

Figure 6. A diagram, viewed down the *a* axis, showing the hydrogen-bonding, marked as red dashed lines, and the π–π stacking interactions (~3.5 Å) in **3**, marked as blue dashed arrows. Hydrogen atoms except for N-H are omitted for clarity.

Asaroidoxazines A (**1**) and B (**2**) represent the third and fourth examples, respectively, of aristolochic acid derivatives that contain oxazinone on the phenanthrene nucleus. They are related to the previously reported aristoloxazines A and B, which were the first aristolochic acid derivatives with an oxazinone moiety isolated from the genus *Aristolochia*.[22] A plausible biosynthetic pathway for **1** and **2** is suggested in Scheme 1. Nitroreduction and intramolecular nucleophilic acyl substitution reaction of aristolochic acid derivatives, which can be biosynthesized from L-tyrosine through benzylisoquinoline alkaloids,[23,24] should give *N*-hydroxydihydrooxazinone intermediates (***i***). The nucleophilic attack of mercaptoacetamide at C-8 of the intermediates (***i***) and the subsequent elimination of *N*-hydroxy group could produce asaroidoxazines A (**1**) and B (**2**).

Scheme 1. Plausible Biosynthetic Pathway for Compounds 1 and 2 in *A. asaroides*

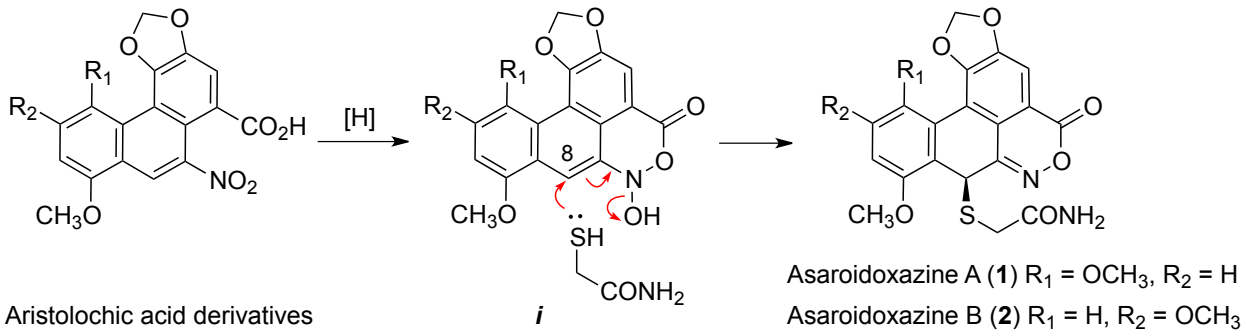

The potential neurotoxicity of compounds **1**–**3** was evaluated in SH-SY5Y human neuroblastoma cells. Asaroidoxazine A (**1**) showed significant neurotoxicity in a concentration-dependent manner, displaying a half-maximum inhibition concentration (IC_{50}) of 2.7 μM, whereas asaroidoxazine B (**2**) and 5-methoxyaristololactam I (**3**) exerted slightly weaker neurotoxicity, with IC_{50} values of 11.2 and 21.2 μM, respectively (Figure 7). To identify the type of cell death induced by asaroidoxazine A (**1**), untreated SH-SY5Y cells (control) and cells treated with asaroidoxazine A (**1**) were stained with Hoechst 33342 (DNA-binding dye) to observe nuclear morphology. The nuclear morphology of the untreated cells remained entirely intact. However, the treated cells showed nuclear condensation and fragmentation (Figure 8A). SH-SY5Y cells treated with asaroidoxazine A (**1**) at the concentrations of 1 and 30 μM, had 36.8% and 70.9% of condensed nuclei, respectively, compared with 2.1% in the untreated cells (Figure 8B). The activity of caspase-3/7, an apoptotic protease, was significantly increased in cells treated with 1 and 30 μM of asaroidoxazine A (**1**) (Figure 8C). In addition, asaroidoxazine A (**1**) decreased intracellular ATP to 57.8% and 51.4% at 1 and 30 μM, respectively, compared with untreated

control (Figure 8D). This indicated that asaroidoxazine A (**1**) treatment causes a moderate ATP reduction. Collectively, these findings revealed that asaroidoxazine A (**1**) is a strong apoptosis inducer in neuroblastoma cells.

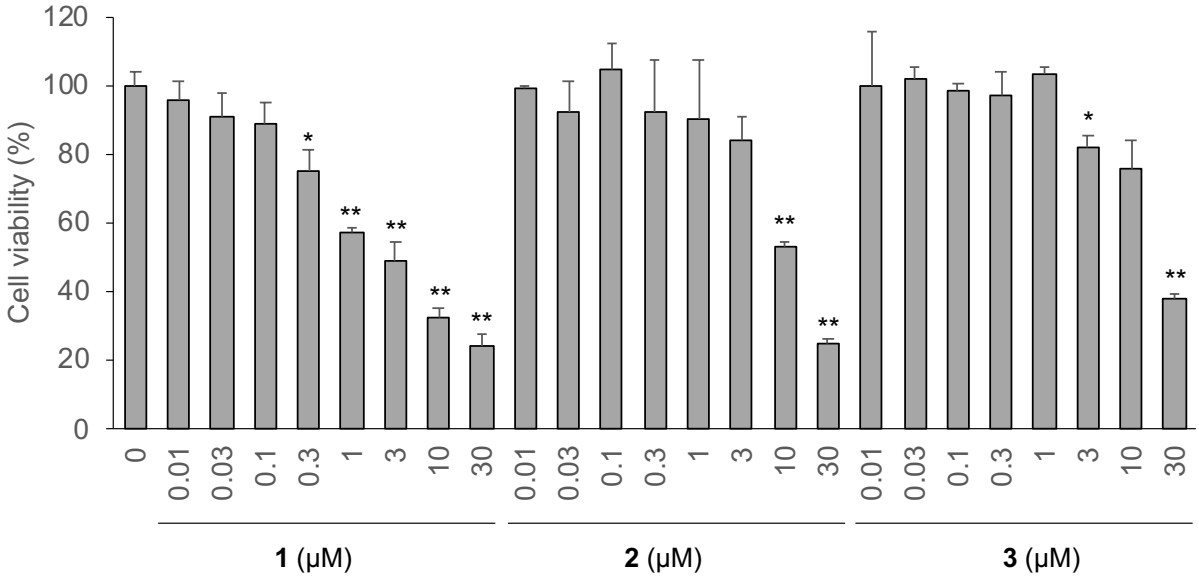

Figure 7. Cell survival rate of SH-SY5Y cells treated or untreated with compounds **1**–**3**. Results are expressed as the means ± SE of three different experiments. **p* <0.05 and ***p* <0.01 from untreated control.

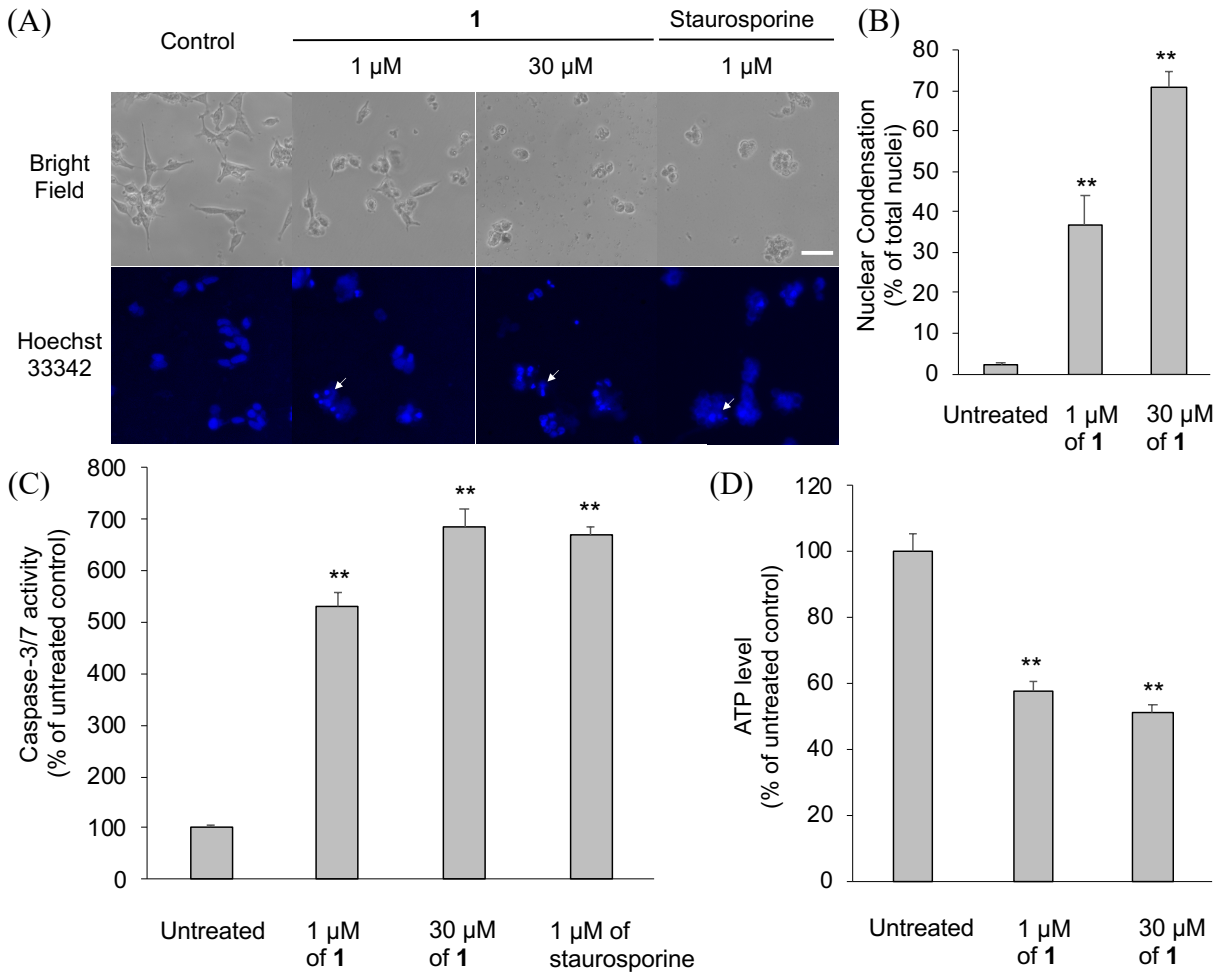

Figure 8. Apoptosis in SH-SY5Y cells induced by compound **1**. (A) Cell morphology of SH-SY5Y cells treated or untreated with compound **1**. Staurosporine (1 μM) was used as the positive control. The examples of the cells with shrunken morphology and condensed or fragmented DNA as visualized by Hoechst 33342 are indicated by white arrows. Bar: 50 μm. (B) Quantification of apoptosis of compound **1**. (C) Caspase-3/7 activity after exposure of SH-SY5Y cells to compound **1** or untreated control for 12 h. Staurosporine (1 μM) was used as the positive control. (D) Effect of compound **1** on ATP level. Results are expressed as the means ± SE of at least three different experiments. ** p <0.01 from untreated control.

Apoptosis or programmed cell death is one of the main mechanisms of cell death in chemotherapy, and natural products play a major role in cancer drug discovery.[25,26] An anthracycline anticancer drug, doxorubicin, is known to interact directly with DNA through the insertion of a mostly planar chromophore between neighboring DNA base pairs. This insertion distorts the polynucleotide structure, resulting in an inhibition of DNA replication and transcription.[27,28] The DNA intercalation by doxorubicin involves the formation of a covalent bond mediated by cellular formaldehyde, between doxorubicin and guanine on one strand of DNA and a hydrogen bond between doxorubicin and guanine on the opposing strand.[29,30] Aristolochic acids with a planar phenanthrene skeleton are known to induce apoptosis in renal tubular cells and embryonic kidney cells 293.[31–34] Furthermore, it has been reported that aristolochic acids can bind to the exocyclic amino groups of purine bases and ultimately form DNA-adducts through an aristolactam nitrenium ion intermediate.[8,35–38] In the present study, asaroidoxazines A (**1**) and B (**2**) were obtained as the first 1,3-dioxolophenanthrene-attached oxazines isolated from the genus *Asarum*. Asaroidoxazine A (**1**) was found to elicit cell death in neuroblastoma cells, characterized through the presentation of typical apoptotic features such as nuclear condensation and caspase activation. Asaroidoxazine A (**1**) has a considerably flattened phenanthrene structure bearing thioether and oxazine functionalities. These structural components are thought to induce neurotoxicity through similar DNA intercalation mechanisms involving formation of DNA-adducts (***iii***) through a nitrenium ion intermediate (***ii***) (Scheme 2). The current findings highlight the potential therapeutic relevance of asaroidoxazine A (**1**) in cancer. Further studies are warranted to delineate the mode of action by which this compound may induce toxicity.

Scheme 2. Possible Mechanism for the Neurotoxicity of Compound 1

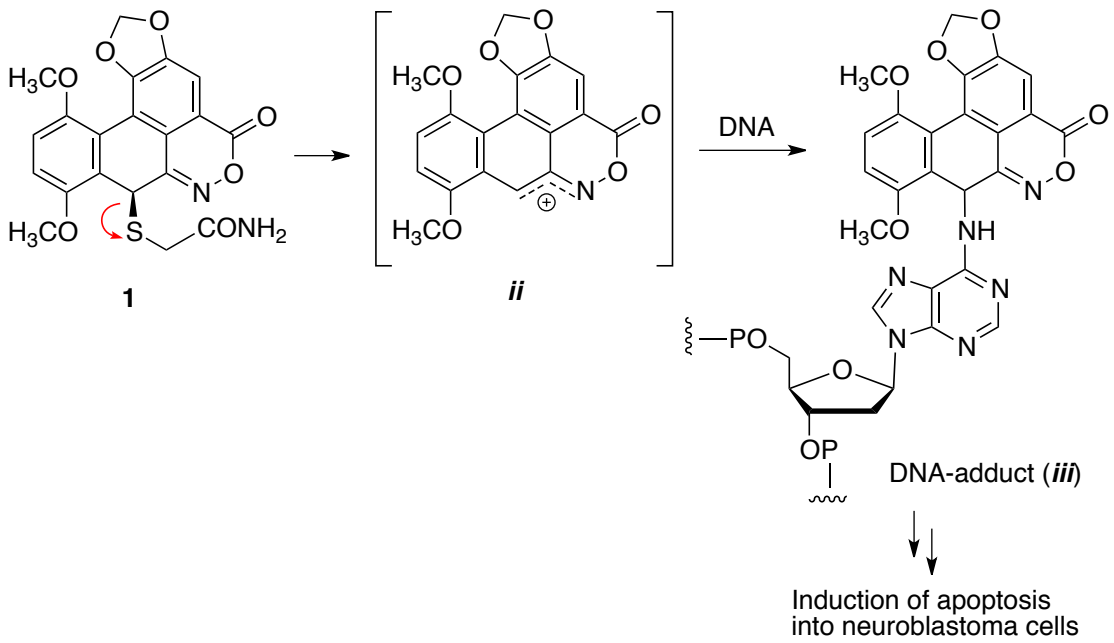

EXPERIMENTAL SECTION

General Experimental Procedures. The melting point was recorded using a Round Science RFS 10 melting point apparatus. Optical rotations were measured on a JASCO P-2200 polarimeter. UV spectra were obtained using a JASCO V-630 Bio spectrophotometer. IR spectra were recorded using a JASCO FT/IR-6300 spectrometer. ECD spectra were measured using a JASCO J-725 spectropolarimeter. NMR spectra were acquired using a JEOL Lambda500 NMR spectrometer (500 MHz for ^{1}H, 125 MHz for ^{13}C). ^{1}H and ^{13}C NMR chemical shifts were referenced to residual solvent peaks (δ_H 7.26 and δ_C 77.0 for $CDCl_3$). HRESIMS were carried out using a Thermo Fisher Scientific LTQ Orbitrap XL mass spectrometer at the Natural Science Center for Basic Research and Development (N-BARD), Hiroshima University. Column chromatography (CC) was

performed using silica gel 60 (40 – 63 μm, Merck). Thin-layer chromatography (TLC) was performed using pre-coated silica gel 60 F_{254} plates (Merck, USA).

Plant Material. *Asarum asaroides* was purchased from Lovely Garden Company (Ehime Prefecture, Japan) in April 2019. The plant was identified by one of the authors (S.O.). A voucher specimen has been deposited at the Hiroshima University Museum, Japan (registry number HUM-PL-00008).

Extraction and Isolation. The roots (32 g) were extracted with MeOH at room temperature for 3 days. The concentrated MeOH extract (0.54 g) was suspended in water and then partitioned successively with *n*-hexane and EtOAc. A portion (0.11 g) of the EtOAc-soluble material (0.13 g) was subjected to silica gel column chromatography eluted with EtOAc–*n*-hexane (0:100, 1:19, 1:9, 1:4, 3:7, 2:3, 1:1, 3:2, 7:3, 4:1, 9:1, 100:0) to obtain 12 fractions. The fractions eluted with EtOAc–*n*-hexane (9:1 and 100:0) (6 mg) was purified by silica gel column chromatography with EtOAc–CH_2Cl_2 (0:100 to 100:0) to afford **1** (1 mg), **2** (0.2 mg), and **3** (0.1 mg).

*Asaroidoxazine A (**1**):* pink crystals; mp 206–208 ˚C; $[\alpha]^{25}_D$ +147 (*c* 0.02, $CHCl_3$); UV (MeOH) λ_{max} (log ε) 210 (4.64), 277 (4.35) nm; IR (KBr) ν_{max} 3410, 1725, 1680, 1615, 1590, 1495, 1463 cm^{-1}; ECD (MeOH) $\Delta\varepsilon_{217}$ –26.4, $\Delta\varepsilon_{288}$ +12.9, $\Delta\varepsilon_{343}$ –3.4; ^1H and ^{13}C NMR data, see Table 1; (+)-HRESIMS *m/z* 451.0569 $[M + Na]^+$ (calcd for $C_{20}H_{17}N_2O_7S^+$, 451.0570).

*Asaroidoxazine B (**2**):* pale yellow oil; $[\alpha]^{25}_D$ +69 (*c* 0.01, $CHCl_3$); UV (MeOH) λ_{max} (log ε) 210 (4.62), 276 (4.32) nm; IR (film) ν_{max} 3430, 1727, 1664, 1631, 1590, 1490, 1472 cm^{-1}; ECD (MeOH) $\Delta\varepsilon_{218}$ –25.8, $\Delta\varepsilon_{290}$ +19.7, $\Delta\varepsilon_{344}$ –2.1; ^1H and ^{13}C NMR data, see Table 1; (+)-HRESIMS *m/z* 429.0753 $[M + H]^+$ (calcd for $C_{20}H_{17}N_2O_7S^+$, 429.0751), 451.0572 $[M + Na]^+$ (calcd for $C_{20}H_{17}N_2O_7S^+$, 451.0570).

X-ray Crystallographic Analysis of 1 and 3. Data collection was performed with a Bruker SMART-APEX II ULTRA CCD area detector with graphite monochromated Mo Kα radiation (λ = 0.71073 Å). The structure was solved by direct methods using SHELXS-97.[39] Refinements were performed with SHELXL-2014/6[40] using full-matrix least squares on F^2. All non-hydrogen atoms were refined anisotropically. The hydrogen atoms of methyl group in the solvent molecule (MeOH) cocrystallized with **1** were placed in idealized positions and refined as riding atoms isotropically. The hydrogen atoms of methoxy groups and bonded to C-6 in **3** were also placed in idealized positions and refined as riding atoms isotropically. The rest of the hydrogen atoms in **1** and **3** were located from difference Fourier maps and their positions and isotropic displacement parameters were refined.

*Crystal Data for **1**.* $C_{21}H_{20}N_2O_8S$, M = 460.45, monoclinic, crystal size, 0.20 x 0.10 x 0.10 mm^3, space group P 21, Z = 2, crystal cell parameters a = 5.0144 (4) Å, b = 11.1979 (9) Å, c = 18.4427 (14) Å, β = 91.2580 (10)˚, V = 1035.32 (14) Å^3, F(000) = 480, Dc = 1.477 Mg/m^3, T = 173 K, 6300 reflections measured, 4615 independent reflections [$R_{(int)}$ = 0.0134], final R indices [I>2.0σ(I)], R_1 = 0.0335, wR_2 = 0.0962, final R indices (all data), R_1 = 0.0372, wR_2 = 0.1018, Flack parameter: 0.05 (3). CCDC-2002419 contains the supplementary crystallographic data for this paper. The data can be obtained free of charge from the Cambridge Crystallographic Data Centre via www.ccdc.cam.ac.uk/data_request/cif.

*Crystal Data for **3**.* $C_{18}H_{13}NO_5$, M = 323.29, triclinic, crystal size, 0.15 x 0.10 x 0.10 mm^3, space group P –1, Z = 4, crystal cell parameters a = 10.618 (3) Å, b = 12.162 (4) Å, c = 13.204 (4) Å, α = 94.952 (5)˚, β = 110.780 (4)˚, γ = 115.495 (4)˚, V = 1380.0 (7) Å^3, F(000) = 672, Dc = 1.556 Mg/m^3, T = 173 K, 6883 reflections measured, 4869 independent reflections [$R_{(int)}$ = 0.0542], final R indices [I>2.0σ(I)], R_1 = 0.0761, wR_2 = 0.1680, final R indices (all data), R_1 =

0.1670, wR_2 = 0.2201, CCDC-2002422 contains the supplementary crystallographic data for this paper. The data can be obtained free of charge from the Cambridge Crystallographic Data Centre via www.ccdc.cam.ac.uk/data_request/cif.

Cell Culture. SH-SY5Y human neuroblastoma cells were purchased from the American Type Culture Collection (CRL-2266; Manassas, VA, USA). Cells were cultured and maintained according to a previous report.[41] Cells were seeded into 12- and/or 96-well plates at a density of 2 × 10^5 cells/well or 2 × 10^4 cells/well, respectively. Cells were used for experiments after 24 h in culture.

Measurement of Cell Viability. Cell viability was evaluated using the Cell Counting Kit-8 (DOJINDO laboratories, Kumamoto, Japan) according to manufacturer's instructions. All experiments were performed in triplicate. Results were expressed as means ± SE of the percentage in the treated cultures compared with those of the untreated cells. Statistical differences were evaluated by Student's *t* test. The IC_{50} was calculated from the non-linear curve fitting of percent inhibition (% inhibition) vs. inhibitor concentration.

Observation of Nuclear Morphology. To evaluate the chromatin condensation and fragmentation, DNA binding fluorochrome Hoechst 33342 was used.[42] Then, 5 μg/mL of Hoechst 33342 were added to each well after treatment and measured fluorescence at 360 ± 40 nm excitation, with a 460 ± 50 nm band-pass filter using a BZ-9000 inverted fluorescent microscope (Keyence, Osaka, Japan). The number of condensed nuclei subsequently was counted with fluorographs.

Measurement of Caspase-3/7 Activity. The caspase-3/7 activity was measured using the Caspase-Glo 3/7 Assay System (Promega, Madison, WI, USA) according to the manufacturer's

instructions. The relative caspase activities were evaluated for the treated cells compared with those of the untreated controls. All experiments were repeated four times. Results were expressed as means ± SE of the percentage in the treated cells compared with those of the untreated cells. Statistical differences were evaluated by the Student's *t* test.

Determination of Intracellular ATP Levels. The intracellular ATP content was measured using the CellTiter-Glo Luminescent Cell Viability Assay Kit (Promega). Known concentrations of ATP were used as standards. All experiments were performed in triplicate. Results were expressed as means ± SE of the percentage in the treated cells compared with those of the untreated cells. Statistical differences were evaluated by the Student's *t* test.

ASSOCIATED CONTENT

Supporting Information

The Supporting information is available free of charge on the ACS Publications webside at DOI: .

- HRMS spectra and NMR spectroscopic data of **1** and **2** (PDF)
- X-ray crystallographic data of **1** (CIF)
- X-ray crystallographic data of **3** (CIF)

AUTHOR INFORMATION

Corresponding Authors

*Tel: +81 82 424 6537. E-mail: ohta@hiroshima-u.ac.jp (S.O.).

*Tel: +81 82 424 6500. E-mail: ishiyasu@hiroshima-u.ac.jp (Y.I.)

ORCID

Shinji Ohta: 0000-0002-1338-5355

Yasuhiro Ishihara: 0000-0001-9751-7660

Notes

The authors declare no competing financial interest.

ACKNOWLEDGMENTS

We thank Mr. Kyo Muranaka and Mr. Yuya Tsubaki, Hiroshima University, for technical assistance. This work was supported in part by JSPS KAKENHI Grant Number 18K05335. We thank Editage (www.editage.com) for English language editing.

REFERENCES

(1) Kelly, L. M. *Amer. J. Bot.* **1998**, *85*, 1454–1467.

(2) Ishikawa N. *Phytochemistry* **1971**, *10*, 3297–3298.

(3) Saiki, Y.; Akahori, Y.; Morinaga, K.; Taira, T.; Noro, T.; Fukushima, S.; Harada, T. *Yakugaku Zasshi* **1967**, *87*, 1544–1547.

(4) Kawamura, T.; Osada, Y.; Okuda, K.; Hisata, Y.; Sakai, E.; Tanaka, T.; Tatematsu, I. *Nat. Med.* **2003**, *57*, 105–109.

(5) Mix, D. B.; Guinaudeau, H.; Shamma, M. *J. Nat. Prod.* **1982**, *45*, 657–666.

(6) Michl, J.; Ingrouille, M. J.; Simmonds, M. S. J.; Heinrich, M. *Nat. Prod. Rep.* **2014**, *31*, 676–693.

(7) Debelle, F. D.; Vanherweghem, J.-L.; Nortier, J. L. *Kidney Int.* **2008**, *74*, 158–169.

(8) Anger, E. E.; Yu, F.; Li, J. *Int. J. Mol. Sci.* **2020**, *21*, 1157.

(9) Dracinska, H.; Barta, F.; Levova, K.; Hudecova, A.; Moserova, M.; Schmeiser, H. H.; Kopka, K.; Frei, E.; Arlt, V. M.; Stiborova, M. *Toxicology* **2016**, *17*, 344–346.

(10) Pistelli, L; Nieri, E.; Bilia, A. R.; Marsili, A.: Scarpato, R. *J. Nat. Prod.* **1993**, *56*, 1605–1608.

(11) Toth, B.; Hohmann, J.; Vasas, A. *J. Nat. Prod.* **2018**, *81*, 661–678.

(12) Wu, T.-S.; Ou, L.-F.; Teng, C.-M. *Phytochemistry* **1994**, *36*, 1063–1068.

(13) Michl, J.; Kite, G. C.; Wanke, S.; Zierau, O.; Vollmer, G.; Neinhuis, C.; Simmonds, M. S. J.; Heinrich, M. *J. Nat. Prod.* **2016**, *79*, 30–37.

(14) Harauchi, Y.; Kajimoto, T.; Ohta, E.; Kawachi, H.; Imamura-Jinda, A.; Ohta, S. *Phytochemistry* **2017**, *43*, 145–150.

(15) Akihara, Y.; Kamikawa, S.; Harauchi, Y.; Ohta, E.; Nehira, T.; Omura, H.; Ohta, S. *Phytochemistry* **2018**, *156*, 151–158.

(16) Xie, B.-B.; Shang, M.-Y.; Lee, K.-H.; Wang, X.; Komatsu, K.; Cai, S-Q. *Nat. Prod. Commun.* **2011**, *6*, 11–14.

(17) Letcher, R. M.; Nhamo, L. R. M. *J. Chem. Soc., Perkin Trans. I* **1972**, 2941–2946.

(18) Flack, H. D. *Acta Cryst.* **1983**, *A39*, 876–881.

(19) Parsons, S.; Flack, H. D.; Wagner, T. *Acta Crystallogr., Sect. B: Struct. Sci., Cryst. Eng. Mater.* **2013**, *B69*, 249–259.

(20) Arreaga-Gonzales, H. M.; Rodriguez-Garcia, G.; del Rio, R. E.; Ferreira-Sereno, J. A.; Garcia-Gutierrez, H. A.; Cerda-Garcia-Rojas, C. M.; Joseph-Nathan, P.; Gemez-Hurtado, M. A. *J. Nat. Prod.* **2019**, *82*, 3394–3400.

(21) Uyama, Y.; Ohta, E.; Harauchi, Y.; Nehira, T.; Omura, H.; Kawacchi, H.; Imamura-Jinda, A.; Uy, M. M.; Ohta, S. *Phytochemistry Lett.* **2020**, *35*, 10–14.

(22) Rios, M. Y.; Navarro, V.; Ramirez-Cisneros, M. A.; Salazar-Rios, E. *J. Nat. Prod.* **2017**, *80*, 3112–3119.

(23) Speck, K.; Magauer, T. *Beilstein J. Org. Chem.* **2013**, *9*, 2048–2078.

(24) dos Santos A. R.; Vaz N. P. In *Sustainable Development and Biodiversity, Vol 24; Biodiversity and Chemotaxonomy*; Ramawat K. G., Ed.; Springer Nature Switzerland AG: Cham, 2019; pp 167–193.

(25) Kawiak, A.; Zawacka-Pankau, J.; Wasilewska, A.; Stasilojc, G.; Bigda, J.; Lojkowska, E. *J. Nat. Prod.* **2012**, *75*, 9–14.

(26) Mortezaee, K.; Najafi, M.; Farhood, B.; Ahmadi, A.; Potes, Y.; Shabeeb, D.; Musa, A. E. *Life Sci.* **2019**, *228*, 228–241.

(27) Box, V. G. S. *J. Mol. Graph. Mod.* **2007**, *26*, 14–19.

(28) Jawad, B.; Poudel, L.; Podgornik, R.; Steinmetz, N. F.; Ching, W.-Y. *Phys. Chem. Chem. Phys.* **2019**, *21*, 3877–3893.

(29) Yang, F.; Teves, S. S.; Kemp, C. J.; Henikoff, S. *Biochim. Biophys. Acta* **2014**, *1845*, 84–89.

(30) Forrest, R. A.; Swift, L. P.; Rephaeli, A.; Nudelman, A.; Kimura, K.-I.; Phillips, D. R.; Cutts, S. M. *Biochem. Pharmacol.* **2012**, *83*, 1602–1612.

(31) Balachandran, P.; Wei, F.; Lin R.-C.; Khan, I. A.; Pasco, D. S. *Kidney Int.* **2005**, *67*, 1797–1805.

(32) Hsin Y.-H.; Cheng, C.-H.; Tzen, J. T. C.; Wu, M.-J.; Shu, K.-H.; Chen, H.-C. *Apoptosis* **2006**, *11*, 2167–2177.

(33) Pozdzik, A. A.; Salmon, I. J.; Debelle, F. D.; Decaestecker, C.; Van den Branden, C.; Verbeelen, D.; Deschodt-Lanckman, M. M.; Vanherweghem, J.-L.; Nortier, J. L. *Kidney Int.* **2008**, *73*, 595–607.

(34) Jadot, I.; Decleves, A.-E.; Nortier, J.; Caron, N. *Int. J. Mol. Sci.* **2017**, *18*, 297.

(35) Stiborova, M.; Fernando, R. C.; Schmeise, H. H.; Frei, E.; Pfau, W.; Wiessier, M. *Carcinogenesis* **1994**, *15*, 1187–1192.

(36) Schmeiser H. H.; Bieler, C. A.: Wiessler, M.; van Ypersele de, S. C.; Cosyns, J. P. *Cancer Res.* **1996**, *56*, 2025–2028.

(37) Priestap, H. A.; de los Santos, C.; Quirke, J. M. E. *J. Nat. Prod.* **2010**, *73*, 1979–1986.

(38) Priestap, H. A.; Barbieri, M. A.; Johnson, F. *J. Nat. Prod.* **2012**, *75*, 1414–1418.

(39) Sheldrick, G. M. *SHELXS-97, Program for Crystal Structure Solution;* University of Göttingen, Göttingen, Germany, 1997.

(40) Sheldrick, G. M. *SHELXL-2014/6, Program for Crystal Structure Refinement;* University of Göttingen, Göttingen, Germany, 2014.

(41) Takemoto, T.; Ishihara, Y.; Ishida, A.; Yamazaki, T. *Environ. Toxicol. Pharmacol.* **2015**, *40*, 199–205.

(42) Ishihara, Y.; Tsuji, M.; Kawamoto, T.; Yamazaki, T. *J. Clin. Biochem. Nutr.* **2016**, *59*, 182–190.